**NASA TECHNICAL MEMORANDUM**

NASA TM X-71604

NASA TM X-71604



# COMPRESSIBLE SEAL FLOW ANALYSIS USING THE FINITE ELEMENT METHOD WITH GALERKIN SOLUTION TECHNIQUE

by John Zuk
Lewis Research Center
Cleveland, Ohio 44135

TECHNICAL PAPER proposed for presentation at
Lubrication Conference sponsored by the
American Society of Mechanical Engineers and the
American Society of Lubrication Engineers
Montreal, Canada, October 8-10, 1974

# Compressible Seal Flow Analysis Using the Finite Element Method With Galerkin Solution Technique

by

John Zuk
NASA-Lewis Research Center

E-5116-2

## ABSTRACT

**High pressure gas sealing involves not only balancing the viscous force with the pressure gradient force but also accounting for fluid inertia--especially for choked flow. The conventional finite element method which uses a Rayleigh-Ritz solution technique is not convenient for nonlinear problems. For these problems, a finite element method with a Galerkin solution technique (FEMGST) was formulated. One example, a three-dimensional axisymmetric flow formulation has nonlinearities due to compressibility, area expansion, and convective inertia. Solutions agree with classical results in the limiting cases. The development of the choked flow velocity profile is shown.**

## Nomenclature

| | |
|---|---|
| $A$ | cross-sectional area, $in.^2$; $m^2$ |
| $a_n$ | basis function geometric coefficient evaluated in Table 2 |
| $A_{\alpha m}^{XY}$ | coefficient expression used in GADE, defined in Table 2 |
| $b_n$ | basis function geometric coefficient evaluated in Table 1 |
| $B_{\alpha\beta m}^{XY}$ | coefficient expression used in GADE, defined in Table 2 |
| $C_j$ | undetermined coefficient |
| $c_n$ | basis function geometric coefficient evaluated in Table 1 |
| $D$ | unknown coefficient matrix |
| $D_{\alpha m}^{XY}$ | coefficient expression used in GADE, defined in Table 2 |
| $E_{\alpha m}^{XY}$ | coefficient expression used in GADE, defined in Table 2 |
| $F_n$ | linear basis function |
| $F_m^{XY}$ | basis function of an element m |
| $\overline{F}_{\alpha m}^{XY}$ | coefficient expression used in GADE, defined in Table 2 |
| $G_{\alpha m}^{XY}$ | coefficient expression used in GADE, defined in Table 2 |
| $h$ | film thickness (gap), in.; m |
| $N$ | total number of mesh points |
| $n$ | an integer |
| $P$ | static pressure, psi; $N/m^2$ |
| $\overline{R}$ | basis function integral defined in Table 4 |
| $\overline{R^2}$ | basis function integral defined in Table 4 |
| $\overline{R^3}$ | basis function integral defined in Table 4 |
| $\overline{RZ}$ | basis function integral defined in Table 4 |
| $\overline{RZ^2}$ | basis function integral defined in Table 4 |

| | |
|---|---|
| $Re$ | leakage flow Reynolds number in radial direction, $\rho Uh/\mu$ |
| $Re^*$ | modified Reynolds number, $Re(h/\Delta R)$ |
| $r$ | radial direction coordinate |
| $r^*$ | dimensionless radial coordinate, $r/\Delta R$ |
| $T$ | temperature, $^{o}F$; K |
| $T^*$ | dimensionless temperature, $T/\Delta T_{ref}$ |
| $U$ | leakage flow reference velocity, ft/sec; m/sec |
| $u$ | velocity in r-direction or x-direction, ft/sec; m/sec |
| $u^*$ | dimensionless velocity, $u/U$ |
| $V$ | dependent variable identification number |
| $V_T$ | number of dependent variable |
| $x$ | coordinate in pressure gradient direction |
| $\overline{Z}$ | basis function integral defined in Table 4 |
| $\overline{Z^2}$ | basis function integral defined in Table 4 |
| $\overline{Z^3}$ | basis function integral defined in Table 4 |
| $\overline{ZR^2}$ | basis function integral defined in Table 4 |
| $z$ | coordinate across film thickness |
| $z^*$ | dimensionless coordinate, $z/h$ |
| $\psi$ | dependent variable |
| $\phi$ | basis function |
| $\Delta$ | area of triangle |
| $\varepsilon$ | error, global or series trunkation |
| $\mu$ | absolute or dynamic viscosity, (lbf)(sec)/in.$^2$; (N)(sec)/m$^2$ |
| $\nu$ | kinematic viscosity, ft$^2$/sec; m$^2$/sec |

$\rho$ density, $(lbf)(sec^2)/in.^4$; $kg/m^3$

$\rho^*$ dimensionless density, $\rho/\rho_0$

$\tau$ shear stress, $lbf/in.^2$; $N/cm^2$

$\{\phi_i F_n\}$ basis function integral defined in Table 3

Subscripts:

i vertex number of triangle element

j vertex number of triangle element or dependent variable number

k vertex number of triangle element

L triangle element identification

m mean or triangle sub-element region

N location along flow leakage length

n vertex number

U triangle element identification

v variable number

x vertex location coordinate, axial direction

y vertex location coordinate, radial direction

$\alpha$ vertex identification of triangle element

$\beta$ vertex identification of triangle element

Superscripts:

X vertex location coordinate, axial direction

Y vertex location coordinate, radial direction

* dimensionless quantity

# INTRODUCTION

A purpose of this paper is to develop a numerical analysis tool which will enable analysis of complex seal problems. The numerical method of solution utilizes a new procedure--the finite element method with a Galerkin solution technique (FEMGST) rather than the method of finite differences. Utilization of this FEMGST should enable the fluid film analysis to be readily integrated with solid mechanics and dynamics finite element analyses which are carried out by existing computer programs. Also, the Galerkin solution procedure can solve nonlinear problems which cannot be solved using the conventional finite element method which uses a Rayleigh-Ritz solution procedure (1).

In pressure balanced face seals and self-acting lift pad seals (2) (Figs. 1 and 2), the flow can choke. Thus fluid inertia must be accounted for in a flow analysis. Since inclusion of fluid inertia makes the flow equations nonlinear, the flow is currently solved using an approximate integrated average model (3).

These approximate seal analyses may not yield satisfactory results when the nonlinearity becomes large. Further, these approximate methods also do not yield detailed distribution information about the flow field. Thus it is necessary to utilize a numerical solution scheme. A finite element method with a Galerkin solution technique is used. A finite difference scheme could have been used. However, it was felt that ultimately a finite element seal flow analysis would be a powerful analysis tool.

Some of the advantages of the finite element method over the finite difference method are:

1. Boundary conditions need not coincide with coordinate lines.

2. Layout of nodal points is more flexible.

3. Boundary conditions of abrupt geometric changes, such as step changes in film thickness, do not require finding a special interfacial boundary condition such as mass flux continuity (4).

4. The method can yield numerical solutions more rapidly. Studies on a transient one-dimensional heat conduction problem show that this method is about six to 60 times faster than the finite difference method, depending on the desired accuracy (5).

The disadvantages of using this method are:

1. The solution is an average value over the element rather than an exact solution at every point in the region; however, this is satisfactory for most engineering problems. Better accuracy can be obtained by decreasing the element size.

2. Programming is also more difficult. A larger software effort may be required.

3. The coefficient matrix for the nonlinear flow problem is non-diagonally dominant due to the momentum equation.

Although seal flow problems, in particular, have not been analyzed using finite element techniques, other lubrication flows have been analyzed using the finite element method. Reddi (4) and (6) has solved some incompressible and compressible bearing lubrication problems using the finite element method with the Rayleigh-Ritz approximate solution procedure. The Reynolds lubrication equation is in quadratic functional

form and thus is an admissible form to a Rayleigh-Ritz solution. Recently Oh and Heubner (7) have applied the finite-element techniques to solve the elastohydrodynamic finite journal bearing problem. The Reynolds' equation for the fluid film and the three-dimensional elasticity equations for the bearing housing were solved simultaneously using an iteration scheme.

The usual finite element method, which is based on a Rayleigh-Ritz approximation, has been extended to other continuum problems such as heat conduction and dynamics (1). This means that a variational principle must be found; e.g., the total potential energy of a system is stationary. However, in fluid mechanics such a principle may not be readily found in a workable form. Also, the classes of nonlinear problems that can be solved are very limited. The problem must be reducible to a quadratic functional. Such problems are described in equations which are sometimes called "quasi-harmonic" equations. The heat conduction equation with variable conductivity, irrotational flow of ideal fluids, Lagrange's equation, and the compressible Reynolds lubrication equation are examples of "quasi-harmonic" equations. The compressible Reynolds' equation, however, neglects convective inertia forces whose retention along with the viscous forces changes the character of the equation so that it is no longer "quasi-harmonic".

The Galerkin method (8) by itself could be used. Cheng and Pan (9) applied Galerkin's method in solving the nonlinear unsteady Reynolds equation. It allowed the reduction of Reynolds equation directly from a partial differencial equation to a system of first-order, ordinary, differential equations, which together with the equations of motion of the journal bearing, yielded a tractable stability analysis of

finite plain journal bearings. Unfortunately, in many problems the series is unworkable when the variables are changing rapidly. Many terms are required in order to have a satisfactory solution. This problem may be overcome by using the Galerkin method with piecewise continuous derivative basis functions. Thus the formulation in this paper is essentially the Galerkin method with finite elements as the basis functions.

## RESULTS AND DISCUSSION

The finite element method with Galerkin solution procedure will be used to solve 3-dimensional axisymmetric and 2-dimensional seal flow problems. An overview of the technique will be presented by outlining the general procedure. The method is basically as follows:

1. Subdivide the region into triangular ring elements as shown in Fig. 3.

2. Define an "irregular pyramid" basis function $F_n(x,y)$ at each nodal point. (A linear basis function - first order splines.) See Fig. 4. Within each triangular element, $F_n$ is a linear function of distance such that $F_n = 1$ at $n = (x,y)$ and $F_n = 0$ on the boundary. Outside of the region defined by the triangular elements touching the point $(x,y)$, $F_n = 0$.

Where: $n$ is the nodal point number, $n = 1,\cdots, N$; $(x,y)$ describe the nodal points in terms of their radial and axial locations. That is, $x$ is the radial direction nodal point number, $x = 1,\cdots, X_{max} = M$, while $y$ is the axial direction nodal point number, $y = 1,\cdots, Y_{max} = N$

3. Let

$$\psi_j(x,y) = \sum_{n=1}^{N} C_{n_j} F_n(x,y) \qquad [1]$$

Where: $j$ is the dependent variable number, $j = 1,\cdots, J$

4. Place the piecewise continuous series into the governing equations.

$$L_i\{\psi_j(x,y)\} = \varepsilon_i \qquad [2]$$

Where: $i$ is the equation number, $i = 1,\cdots, J$

5. Orthogonalize the global error to each basis function as required by the Galerkin method.

$$\int_A \varepsilon_i F_n \, dA = 0$$

6. Place the boundary conditions on the appropriate nodal points.

7. Solve the resulting NJ linear or nonlinear algebraic equations for NJ unknowns.

The details of the finite element method with Galerkin solution technique will now be discussed. The domain of interest is subdivided into triangular subregions as seen in Fig. 3 (a plan view of the r-z plane). Consider a triangular subregion with vertices i, j, and k as seen in Fig. 5.

Let the dependent variables $\psi_1, \psi_2, \psi_3, \cdots \psi_V$ be linearly varying in this triangular subregion; i.e., let

$$\begin{aligned} \psi_1 &= a_1 + b_1 r + c_1 z \\ \psi_2 &= a_2 + b_2 r + c_2 z \\ &\vdots \\ \psi_V &= a_V + b_V r + c_V z \end{aligned} \qquad [3]$$

The linearly varying field assures continuity between elements since "lines which are initially straight remain straight in their displaced position". The nodal or vertex values of $\psi_V$ are defined uniquely and continuously throughout the region; however, the first derivative is discontinuous, hence, this function with piecewise continuous derivatives is a first order spline. At the nodal points of any triangular element, a dependent variable can be expressed as

$$\psi_{1i} = a_1 + b_1 r_i + c_1 z_i$$

$$\psi_{1j} = a_1 + b_1 r_j + c_1 z_j \qquad [4]$$

$$\psi_{1k} = a_1 + b_1 r_k + c_1 z_k$$

which in matrix form becomes

$$\{\psi_{1_n}\} = [D]\{\alpha\} \qquad [5]$$

or

$$\{\alpha\} = [D]^{I}\{\psi_{1_n}\} \qquad [6]$$

where

$$\{\alpha\} = \begin{Bmatrix} a_1 \\ b_1 \\ c_1 \end{Bmatrix} \qquad [7]$$

Hence, the unknown coefficients from Eq. [1] have been expressed in terms of the vertex position and dependent variable values at these nodal (vertex) points. The inversion of the coefficient matrix, [D], is shown in (10). Hence, it can be readily shown that the resulting form of the dependent variable in a triangular subregion m is:

$$\psi_{V(m)} = \frac{1}{2\Delta_m}\Big[(a_i + b_i r + c_i z)\psi_{vi} + (a_j + b_j r + c_j z)\psi_{vj} + (a_k + b_k r + c_k z)\psi_{vk}\Big]_m \qquad [8]$$

The values for a, b, and c are shown in Table I. The basis function can also be expressed in the above form. The basis function equation is developed in (10) and is

$$F_n = \frac{1}{2\Delta}\ (a_i + b_i r + c_i z)F_i + (a_j + b_j r + c_j z)F_j + (a_k + b_k r + c_k z)F_k \qquad [9]$$

where the basis function may have one of the following combinations:

$$\{F_i = 1,\ F_j = 0,\ F_k = 0\},\ \{F_i = 0,\ F_j = 1,\ F_k = 0\},\ \{F_i = 0,\ F_j = 0,\ F_k = 1\} \qquad [10]$$

A given basis function whose value is unity at nodal point XY, will have an irregular pyramid's base as its region of definition. The convention that is used results in six member triangular subelements - which comprise the region of definition of a basis function located at an interior mesh point. See Fig. 5.

$$F_n = \left[\frac{a_j + b_j r + c_j z}{2\Delta}\right]_{L-1} + \left[\frac{a_k + c_k z}{2\Delta}\right]_{L} + \left[\frac{a_k + b_k r}{2\Delta}\right]_{L+1} + \left[\frac{a_j + b_j r}{2\Delta}\right]_{U-1} + \left[\frac{a_i + c_i z}{2\Delta}\right]_{U} + \left[\frac{a_i + b_i r + c_i z}{2\Delta}\right]_{U+1} \qquad [11]$$

As previously described, the piecewise continuous derivative representation of each dependent variable, [8], is placed into the governing Eq. [2]

$$L_i\{\psi_j(x,y)\} = r_i$$

Then the global error is orthogonalized to each basis function as required by the Galerkin method, Eq. [3]

$$\int_A \varepsilon_i F_n dA = 0$$

Since the basis functions, $F_n$, are zero outside of the irregular base pyramid region, Eq. [3] can be written as

$$\sum_{n=(X,Y)=(1,1)}^{M,N} \int_A \varepsilon_i F_n dA = 0 \qquad [12]$$

Thus, a term of the sum in [12] becomes the following for the basis function that has a value of unity at $n = X,Y$, the apex of the pyramid.

$$\int_{L-1} \varepsilon_i F_{xy} dA + \int_L \varepsilon_i F_{xy} dA + \int_{L+1} \varepsilon_i F_{xy} dA + \int_{U-1} \varepsilon_i F_{xy} dA$$

$$+ \int_U \varepsilon_i F_{xy} dA + \int_{U+1} \varepsilon_i F_{xy} dA = 0 \qquad [13]$$

At a point of any triangular region of the pyramid base, a dependent variable is influenced by the values at its vertices. This can be expressed as

$$\psi = C_i F_i + C_j F_j + C_k F_k \qquad [14]$$

Since $C_i = \psi_i$, etc., Eq. [14] can be expressed as

$$\psi = F_i\psi_i + F_j\psi_j + F_k\psi_k$$

where: $F_i$, $F_j$, $F_k$ are basis functions that have the apex = unity at vertices i, j, k, respectively; $\psi_i$, $\psi_j$, $\psi_k$ are the magnitudes of the basis vectors which describe the plane (equal to the magnitude of the variable at the vertex).

By utilizing linear basis functions, the resultant solution vector (where the coefficients have been determined) describing the triangular plane will remain a plane; at the interface of the triangular element (boundaries) the functions are continuous but not the derivatives (since the basis function is a first order spline). The whole volume of each basis function can be geometrically interpreted as an irregular hexagonal based pyramid function.

See Fig. 5 for a plan view of the region of definition of a typical basis function, $F_n$. Fig. 6 illustrates a 3-dimensional geometric interpretation of the function space. Note, the bases are irregular to show a variable mesh situation.

## SEAL FLOW EQUATION FORMULATION

The compressible seal leakage flow will not be analyzed using the finite element method with Galerkin solution technique (FEMGST). The proper dimensionless governing equations where "quasi-fully developed", parallel flow exists, using shear stress as a dependent variable, are:

1. Conservation of mass

$$\frac{\partial}{\partial r^*}(\rho^* r^* u^*) = 0 \qquad [15]$$

2. Conservation of momentum

$$Re^* \rho^* u^* \frac{\partial u^*}{\partial r^*} + \frac{\partial P^*}{\partial r^*} - \frac{\partial \tau^*}{\partial z^*} = 0 \qquad [16]$$

3. Perfect gas relation

$$\rho^* T^* - P^* = 0 \qquad [17]$$

4. Shear stress-velocity relation

$$\frac{\partial u^*}{\partial z^*} - \tau^* = 0 \qquad [18]$$

where

$$Re^* = Re_1 \left( \frac{h}{R_2 - R_1} \right)$$

Only isothermal flow cases will be considered.

### FEMGST Form of Equations

The procedure for forming the Galerkin approximation equations for the above set of partial differential equations will not be presented using the procedure described in the previous section. Details of this procedure can be found in (10).

The equations governing isothermal compressible leakage flow in FEMGST form at nodal point XY are

1. Conservation of mass

$$\sum_{m=L-1}^{U+1} \left[ D^{XY}_{\alpha m} \left( \frac{b_\gamma}{2\Delta_m} \right) \rho_\gamma u_\alpha + B^{XY}_{\alpha\beta m} u_\alpha \rho_\beta + D^{XY}_{\alpha m} \left( \frac{b_\gamma}{2\Delta_m} \right) u_\gamma \rho_\alpha \right] = 0 \qquad [19]$$

2. Conservation of momentum

$$\sum_{m=L-1}^{U+1} \left[ Re^* \left( \frac{b_\gamma}{2\Delta_m} \right) u_\gamma B^{XY}_{\alpha\beta m} u_\alpha \rho_\beta + E^{XY}_{\alpha m} P_\alpha - \underline{F}^{XY}_{\alpha m} \tau_\alpha \right] = 0 \qquad [20]$$

3. Shear stress-velocity relation

$$\sum_{m=L-1}^{U+1} \left( \underline{F}^{XY}_{\alpha m} u_\alpha - A^{XY}_{\alpha m} \tau_\alpha \right) = 0 \qquad [21]$$

4. Equation of state

$$\sum_{m=L-1}^{U+1} \left( B^{XY}_{\alpha\beta m} \rho_\alpha T_\beta - A^{XY}_{\alpha m} P_\alpha \right) = 0 \qquad [22]$$

The functions $A^{XY}_{\alpha m}$, $B^{XY}_{\alpha\beta m}$, $D^{XY}_{\alpha m}$, $E^{XY}_{\alpha m}$, $F^{XY}_{\alpha m}$, and $G^{XY}_{\alpha m}$ are defined in Tables 2, 3 and 4.

A typical seal flow region subdivided into triangular ring elements is shown in Fig. 3. The flow is treated as axisymmetric. Basically, FEMGST is the Galerkin method with finite elements as basis functions. As previously mentioned, at each nodal point an "irregular pyramid" basis function $F_n(r,z)$ is defined (see Fig. 4).

## DISCUSSION

As a starting point, the first case studied in detail was incompressible radial Poiseuille flow. This flow is simpler in nature than the cases of interest. For this case Eqs. [15], [16], and [18] are solved with $Re^* = 0$ and $\rho^* = 1$.

Figure 7 shows the model and conditions used for solving incompressible radial Poiseuille flow. Figures 8, 9, and 10 compare the numerical solutions with the exact analytical solutions at various radial locations for velocity, pressure, and shear stress, respectively. Note, there is excellent agreement for the mesh size chosen.

In order to check the compressible flow formulation of FEMGST, a special inviscid flow problem was solved. The modified Reynolds number $Re^*$ was a parameter varied in this study. The inviscid flow problem had all of the salient features of the general compressible flow seal leakage problem. That is, nonlinearity due to compressibility, area expansion, and convective inertia. However, the problem is simplified because the shear stress is everywhere zero. The radial velocity distribution is shown in Fig. 11. There is excellent agreement between the exact and FEMGST solutions.

A compressible seal flow case of practical interest was then solved. A seal was studied with a radius ratio of 0.8 (see Fig. 12). The transverse velocity profiles at the seal exit are shown in Fig. 13, whereas the radial pressure distributions at the dimensionless transverse gap value of 0.25 are shown in Fig. 14. The modified Reynolds number again was a parameter, but its value here is a measure of the convective inertia effect in the flow. For $Re^* = 0$ the results can

be compared with the exact viscous compressible flow solution. Note the good agreement of FEMGST with the exact solution. For $Re^* \neq 0$ there is no exact solution for comparison; however, the results are physically expected. The solutions were terminated at $Re^* = 12$. At $Re^* = 12$, the results indicate that the limiting exit sonic velocity conditions had been reached at the centerline. The solution had to be terminated because results indicated that the formulated set of equations was no longer valid. The radial pressure distribution in Fig. 14 shows that the exit pressures change the most with Reynolds number. This is expected; since the velocity increase is the greatest in the exit region, the density (pressure for this isothermal case) must correspondingly decrease. This can be seen by examining the compressibility terms in the mass conservation equation.

To use FEMGST, a new computer technique had to be developed. The system of equations from FEMGST could not be solved by the usual iterative solution methods. Thus, a direct method algorithm was developed and used to reduce the large, sparse, nonsymmetric band matrix. This method greatly reduced machine storage requirements and is described in (10).

## REFERENCES

1. Zienkiewicz, O. C. The Finite Element Method in Engineering Science, McGraw-Hill, 2nd, ed., New York, 1971.

2. Zuk, J., Ludwig, L. P., and Johnson, R. L., "Design Study of Shaft Face Seal With Self-Acting Lift Augmentation, I-- Self-Acting Pad Geometry", NASA TN D-5744, 1970.

3. Zuk, J., Ludwig, L. P., and Johnson, R. L., "Compressible Flow Across Shaft Face Seals", Paper FICFS-H6, Fifth International Conference on Fluid Sealing, 1971.

4. Reddi, M. M., "Finite-Element Solution of the Incompressible Lubrication Problem", Journal of Lubrication Technology, Trans. ASME, Series F, Vol. 91, July 1969, pp. 524-533.

5. Price, H. S. and Varga, R. S.. Error Bounds for Semi-Discrete Galerkin Approximations of Parabolic Problems with Applications to Petroleum Reservoir Mechanics. AEC report AT911-1)-1702.

6. Reddi, M. M., and Chu, T. Y., "Finite Element Solution of the Steady-State Compressible Lubrication Problem. Journal of Lubrication Technology, Trans. ASME, Series F, Vol. 92, July 1970, pp. 495-503.

7. Oh, K. P., and Huebner, K. H., "Solution of the Elastohydrodynamic Finite Journal Bearing Problem", Journal of Lubrication Technology, Trans. ASME, Series F, Vol. 95, April 1973, pp. 342-352.

8. Kantorvich, L. V., and Krylov, V. I., Approximate Methods of Higher Analysis, 3rd edition, Interscience, New York, 1958.

9. Cheng, H. S., and Pan, C. H. T.: Stability Analyisi of Gas-Lubricated, Self-Acting, Plain, Cylindrical, Journal Bearings of Finite Length,

Using Galerkin's Method. Journal of Basic Engineering, Trans. ASME, Ser. D, Vol. 85, March 1965, 185-192.

10. Zuk, J., "Fluid Mechanics of Noncontacting Gas Film Seals", PhD Thesis, Cast Western Reserve University, 1972.

**Table I. - Values of Geometric Basis Function Coefficients**

| | | |
|---|---|---|
| $a_i = r_j z_k - r_k z_j$ | $a_j = r_k z_i - r_i z_k$ | $a_k = r_i z_j - r_j z_i$ |
| $b_i = z_j - z_k$ | $b_j = z_k - z_i$ | $b_k = z_i - z_j$ |
| $c_i = r_k - r_j$ | $c_j = r_i - r_k$ | $c_k = r_j - r_i$ |

**Table II.** - Coefficient Expressions Used in Galerkin Approximation Difference Form (GADE)

| Variable Form | GADE Form |
|---|---|
| $\frac{\partial \psi_\alpha}{\partial r}$ | $E^{XY}_{\alpha m} = \frac{b_\alpha}{2\Delta_m}\left\{F^{XY}_m\right\}$ |
| $\frac{\partial \psi_\alpha}{\partial z}$ | $F^{XY}_{\alpha m} = \frac{c_\alpha}{2\Delta_m}\left\{F^{XY}_m\right\}$ |
| $\psi_\alpha$ | $A^{XY}_{\alpha m} = \frac{1}{2\Delta_m}\left(a_\alpha\left\{F^{XY}_m\right\} + b_\alpha\left\{rF^{XY}_m\right\} + c_\alpha\left\{ZF^{XY}_m\right\}\right)$ |
| $\frac{\partial}{\partial r}(r\psi_\alpha)$ | $G^{XY}_{\alpha m} = \frac{1}{2\Delta_m}\left(a_\alpha\left\{F^{XY}_m\right\} + 2b_\alpha\left\{rF^{XY}_m\right\} + c_\alpha\left\{ZF_m\right\}\right)$ |
| $r\psi_\alpha$ | $D^{XY}_{\alpha m} = \frac{1}{2\Delta_m}\left(a_\alpha\left\{rF^{XY}_m\right\} + b_\alpha\left\{r^2F^{XY}_m\right\} + c_\alpha\left\{rzF^{XY}_m\right\}\right)$ |
| $\psi_\alpha\psi_\beta$ | $B^{XY}_{\alpha\beta m} = \frac{1}{4\Delta_m^2}\left(a_\alpha a_\beta\left\{F^{XY}_m\right\} + a_\alpha b_\beta\left\{rF^{XY}_m\right\} + a_\alpha c_\beta\left\{zF^{XY}_m\right\} + b_\alpha c_\beta\left\{rzF^{XY}_m\right\} + b_\alpha b_\beta\left\{r^2F^{XY}_m\right\} + c_\alpha c_\beta\left\{Z^2F^{XY}_m\right\} + a_\beta b_\alpha\left\{rF^{XY}_m\right\} + a_\beta c_\alpha\left\{zF^{XY}_m\right\} + b_\beta c_\alpha\left\{r_zF^{XY}_m\right\}\right)$ |
| $\psi_\alpha \frac{\partial \psi_\beta}{\partial r}$ | $\frac{b_\beta A^{XY}_{\alpha m}}{2\Delta_m} = \frac{b_\beta}{4\Delta_m^2}\left(a_\alpha\left\{F^{XY}_m\right\} + b_\alpha\left\{rF^{XY}_m\right\} + c_\alpha\left\{zF^{XY}_m\right\}\right)$ |

Note: $r\psi_\alpha \frac{\partial \psi_\beta}{\partial r} = \frac{rb_\beta A^{XY}_{\alpha m}}{2\Delta_m} = \frac{b_\beta}{2\Delta_m} D^{XY}_{\alpha m}$

**Table III. –** Basis Function Integrals For a Basis Function Whose Apex (Unit Value) is at Nodal Point $\alpha$

1. L-1 Element; $\alpha = j$, therefore, $F_j = 1$

$$\left\{F^{XY}_{L-1}\right\} = \frac{1}{2\Delta_{L-1}}\left[a_j\Delta_{L-1} + b_j\overline{R} + c_j\overline{Z}\right]$$

$$\left\{rF^{XY}_{L-1}\right\} = \frac{1}{2\Delta_{L-1}}\left[a_j\overline{R} + b_j\overline{R^2} + c_j\overline{RZ}\right]$$

$$\left\{zF^{XY}_{L-1}\right\} = \frac{1}{2\Delta_{L-1}}\left[a_j\overline{Z} + b_j\overline{RZ} + c_j\overline{Z^2}\right]$$

$$\left\{rzF^{XY}_{L-1}\right\} = \frac{1}{2\Delta_{L-1}}\left[a_j\overline{RZ} + b_j\overline{R^2Z} + c_j\overline{RZ^2}\right]$$

$$\left\{r^2F^{XY}_{L-1}\right\} = \frac{1}{2\Delta_{L-1}}\left[a_j\overline{R^2} + b_j\overline{R^3} + c_j\overline{R^2Z}\right]$$

$$\left\{z^2F^{XY}_{L-1}\right\} = \frac{1}{2\Delta_{L-1}}\left[a_j\overline{Z^2} + b_j\overline{RZ^2} + c_j\overline{Z^3}\right]$$

Repeat above calculations for:

2. L Element; except $\alpha = k$, $F_k = 1$

3. L + 1 Element; except $\alpha = k$, $F_k = 1$

4. U - 1 Element; except $\alpha = j$, $F_j = 1$

5. U Element; except $\alpha = i$, $F_i = 1$

6. U + 1 Element; except $\alpha = i$, $F_i = 1$

**Table IV. - Values of Basis Function Integrals**

$$\overline{R} = \iint r\,dr\,dz = d_r \Delta$$

$$\overline{Z} = \iint z\,dr\,dz = d_z \Delta$$

$$\overline{R^2} = \iint r^2\,dr\,dz = \frac{\Delta}{12}\left(\overline{r}_i^2 + \overline{r}_j^2 + \overline{r}_k^2\right) + \Delta d_{rm}^2$$

$$\overline{Z^2} = \iint z^2\,dr\,dz = \frac{\Delta}{12}\left(\overline{z}_i^2 + \overline{z}_j^2 + \overline{z}_k^2\right) + \Delta d_{zm}^2$$

$$\overline{RZ} = \iint r_z\,dr\,dz = \frac{\Delta}{12}\left(\overline{r}_i \overline{z}_i + \overline{r}_j \overline{z}_j + \overline{r}_k \overline{z}_k\right) + \Delta d_{rm} d_{zm}$$

$$\overline{R^3} = \iint r^3\,dr\,dz$$

$$\overline{R^2 Z} = \iint r^2 z\,dr\,dz$$

$$\overline{RZ^2} = \iint r z^2\,dr\,dz$$

$$\overline{Z^3} = \iint z^3\,dr\,dz$$

$$\Delta = \iint dr\,dz = \frac{1}{2}\begin{vmatrix} 1 & r_i & z_i \\ 1 & r_j & z_j \\ 1 & r_k & z_k \end{vmatrix}$$

$$\int_{\Delta} z^3 dzdr = \frac{1}{4}\left[A^4_{ki}(r_k - r_i) + A^4_{jk}(r_j - r_k) + A^4_{ij}(r_i - r_j)\right.$$

$$+ 2A^3_{ki}B_{ki}(r^2_k - r^2_i) + 2A^3_{jk}B_{jk}(r^2_j - r^2_k) + 2A^3_{ij}B_{ij}(r^2_i - r^2_j)$$

$$+ 2A^2_{ki}B^2_{ki}(r^3_k - r^3_i) + 2A^2_{jk}B^2_{jk}(r^3_j - r^3_k) + 2A^2_{ij}B^2_{ij}(r^3_i - r^3_j)$$

$$+ A_{ki}B^3_{ki}(r^4_k - r^4_i) + A_{jk}B^3_{jk}(r^4_j - r^4_k) + A_{ij}B^3_{ij}(r^4_i - r^4_j)$$

$$\left. + \frac{1}{5}B^4_{ki}(r^5_k - r^5_i) + \frac{1}{5}B^4_{jk}(r^5_j - r^5_k) + \frac{1}{5}B^4_{ij}(r^5_i - r^5_j)\right] = \overline{Z^3}$$

$$\int_{\Delta} z^2 r dzdr = \frac{1}{3}\left[\frac{1}{2}A^3_{ki}(r^2_k - r^2_i) + \frac{1}{2}A^3_{jk}(r^2_j - r^2_k) + \frac{1}{2}A^3_{ij}(r^2_i - r^2_j)\right.$$

$$+ A^2_{ki}B_{ki}(r^3_k - r^3_i) + A^2_{jk}B_{jk}(r^3_j - r^3_k) + A^2_{ij}B_{ij}(r^3_i - r^3_j)$$

$$+ \frac{3}{4}A_{ki}B^2_{ki}(r^4_k - r^4_i) + \frac{3}{4}A_{jk}B^2_{jk}(r^4_j - r^4_k)$$

$$+ \frac{3}{4}A_{ij}B^2_{ij}(r^4_i - r^4_j) + \frac{1}{5}B^3_{ki}(r^5_k - r^5_i) + \frac{1}{5}B^3_{jk}(r^5_j - r^5_k)$$

$$\left. + \frac{1}{5}B^3_{ij}(r^5_i - r^5_j)\right] = \overline{Z^2 R}$$

**Table IV. -** Continued

$$\int_{\Delta} zr^2 dzdr = \frac{1}{2}\left[\frac{1}{3} A_{ki}^2 (r_k^3 - r_i^3) + \frac{1}{3} A_{jk}^2 (r_j^3 - r_k^3) + \frac{1}{3} A_{ij}^2 (r_i^3 - r_j^3)\right.$$

$$+ \frac{1}{2} A_{ki} B_{ki} (r_k^4 - r_i^4) + \frac{1}{2} A_{jk} B_{jk} (r_j^4 - r_k^4)$$

$$+ \frac{1}{2} A_{ij} B_{ij} (r_i^4 - r_j^4) + \frac{1}{5} B_{ki}^2 (r_k^5 - r_i^5) + \frac{1}{5} B_{jk}^2 (r_j^5 - r_k^5)$$

$$\left. + \frac{1}{5} B_{ij}^2 (r_i^5 - r_j^5)\right] = \overline{ZR^2}$$

$$\int_{\Delta} r^3 dzdr = \left[\frac{1}{4} A_{ki} (r_k^4 - r_i^4) + \frac{A_{jk}}{4} (r_j^4 - r_i^4) + \frac{A_{ij}}{4} (r_i^4 - r_j^4)\right.$$

$$+ \frac{1}{5} B_{ki} (r_k^5 - r_i^5) + \frac{1}{5} B_{jk} (r_j^5 - r_k^5)$$

$$\left. + \frac{1}{5} B_{ij} (r_i^5 - r_j^5)\right] = \overline{R^3}$$

where:

$$d_z = \frac{z_i + z_j + z_k}{3}; \qquad d_r = \frac{r_i + r_j + r_k}{3}$$

$$A_{ij} = \frac{r_i z_j - r_j z_i}{r_i - r_j} = \frac{a_k c_i c_j}{-c_k}; \qquad A_{jk} = \frac{r_j z_k - r_k z_j}{r_j - r_k} = \frac{a_i c_j c_k}{-c_i}$$

$$B_{ij} = \frac{z_i - z_j}{r_i - r_j} = \frac{b_k c_i c_j}{-c_k}; \qquad B_{jk} = \frac{z_j - z_k}{r_j - r_k} = \frac{b_i c_j c_k}{-c_i}$$

$$A_{ki} = \frac{r_k z_i - r_i z_k}{r_k - r_i} = \frac{a_j c_i c_k}{-c_j}; \qquad B_{ki} = \frac{z_k - z_i}{r_k - r_i} = \frac{b_j c_i c_k}{-c_j}$$

Table IV. - Continued

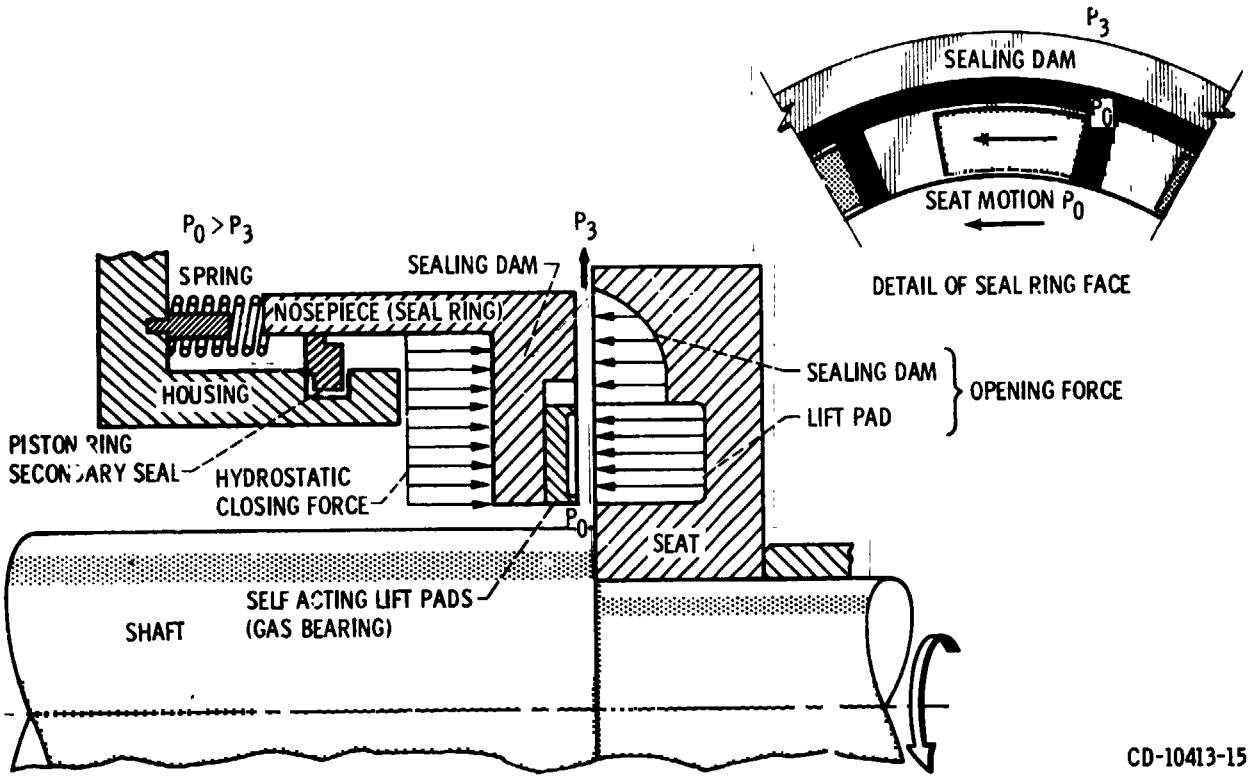


E-5116-2

Figure 1. - Pressure-balanced face seal with self-acting lift pads (added for axial film stiffness).

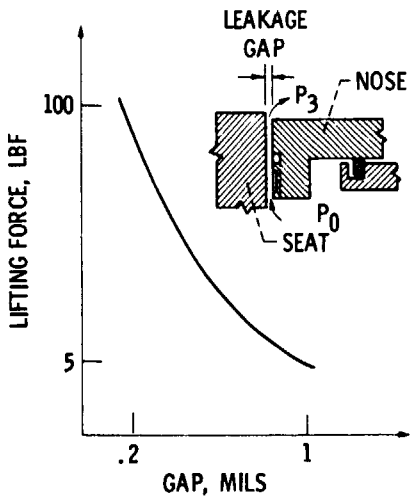


Figure 2. - Gas bearing for seal support.

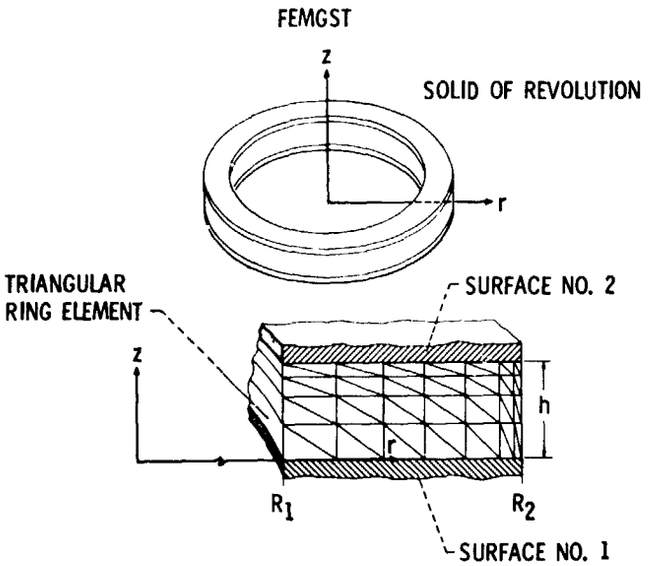


Figure 3. - The finite element idealization of flow through a gas film seal.

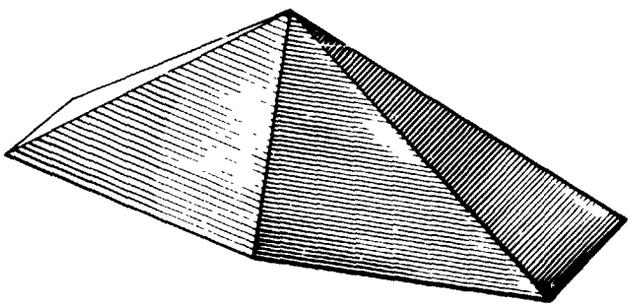

(a) THREE-DIMENSIONAL REPRESENTATION OF THE BASIS FUNCTION.

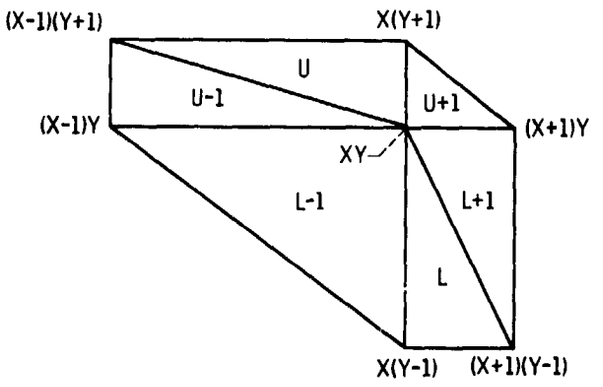


(b) BASE OF IRREGULAR PYRAMID USED TO DEFINE BASIS FUNCTION.

Figure 4. - Geometric interpretation of an irregular hexagonal based pyramid function.

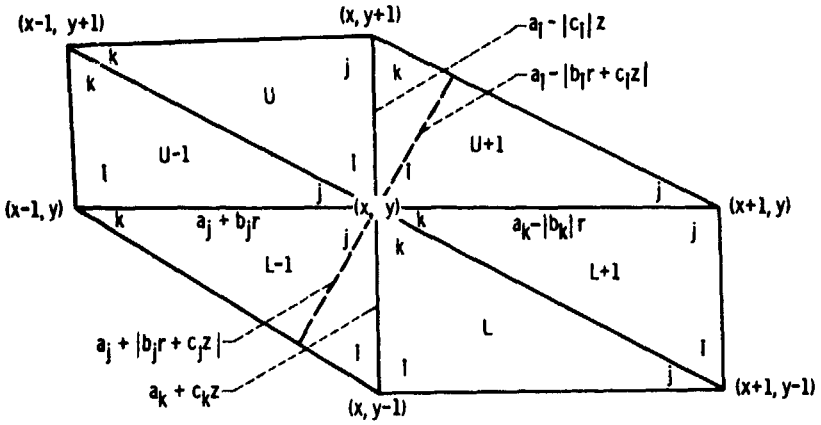


Figure 5. - General pattern of irregular pyramid basis function (IHBPF).

E-5116-2

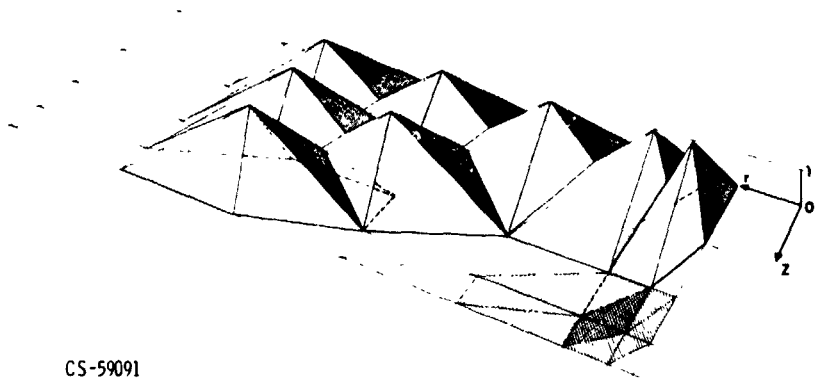


CS-59091

Figure 6. - Geometric interpretation of function space (irregular hexagonal based pyramid basis functions).

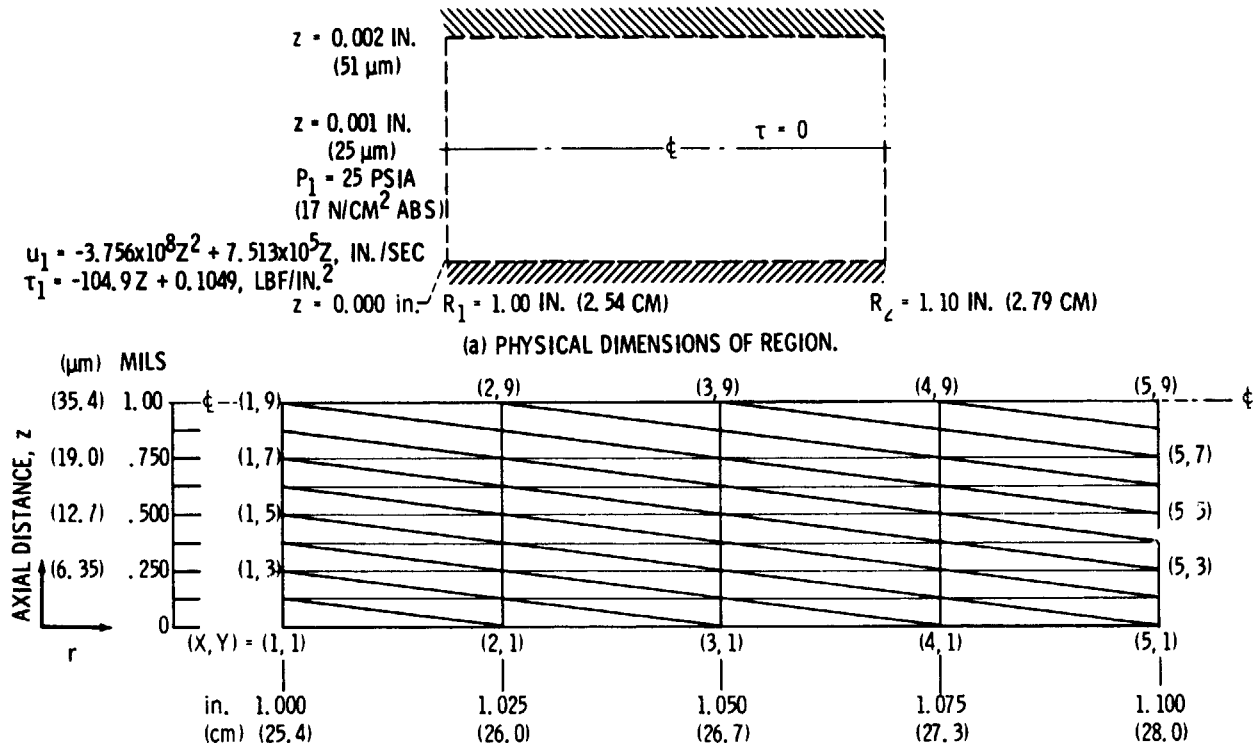


Figure 7. - Incompressible radial Poiseuille flow sample problem.

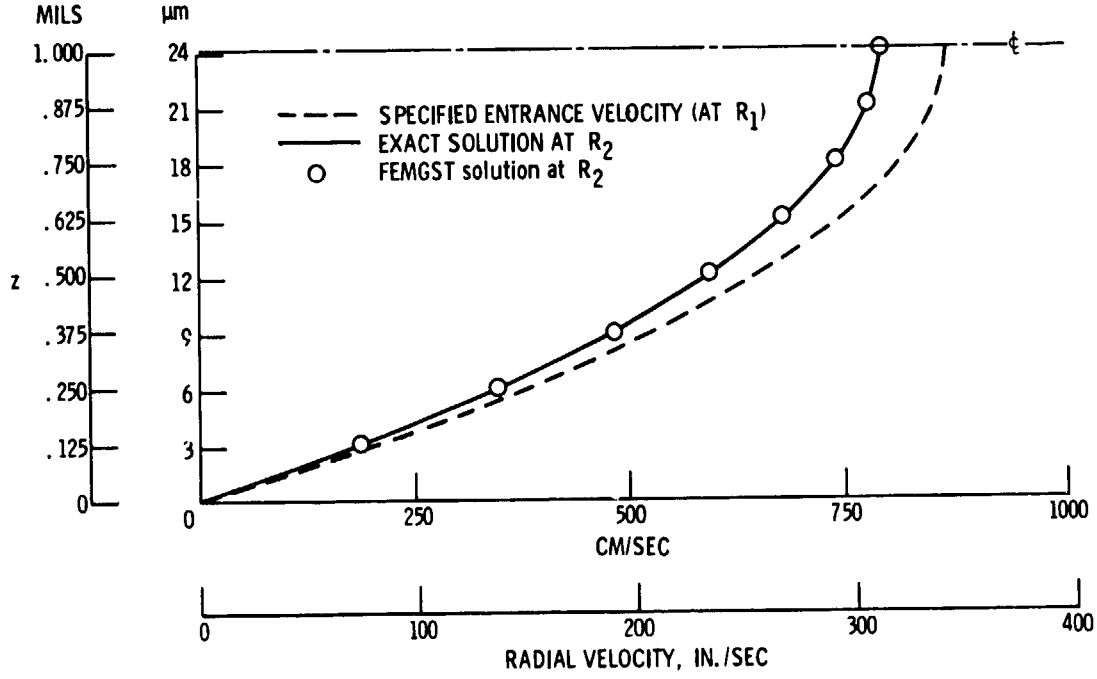


Figure 8. - Comparison of FEMGST solution with exact solution for radial velocity distribution.

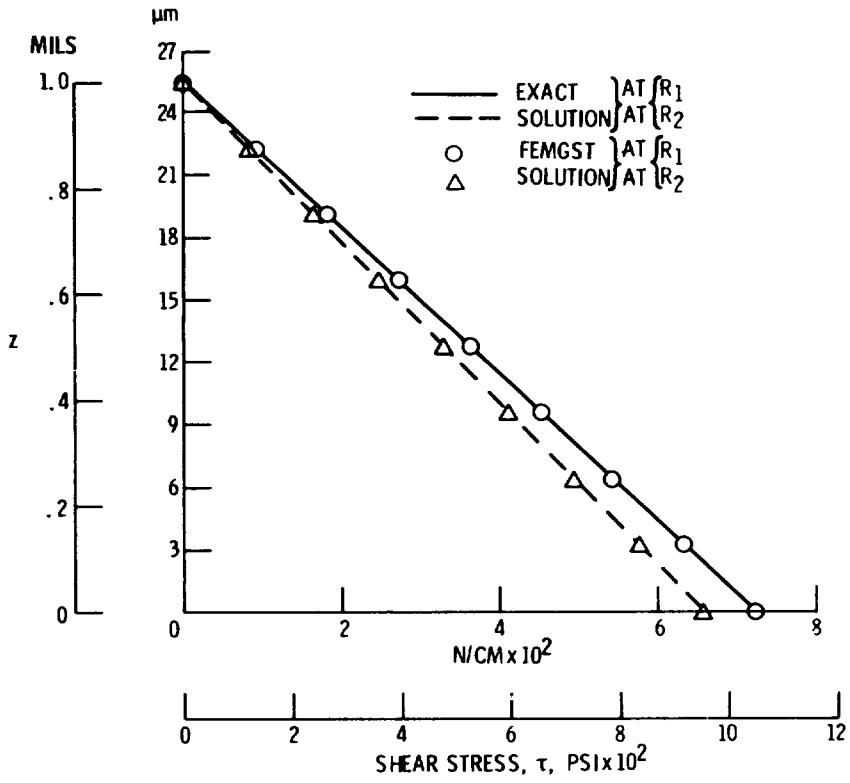


Figure 9. - Comparison of FEMGST solution with exact solution for shear stress distribution.

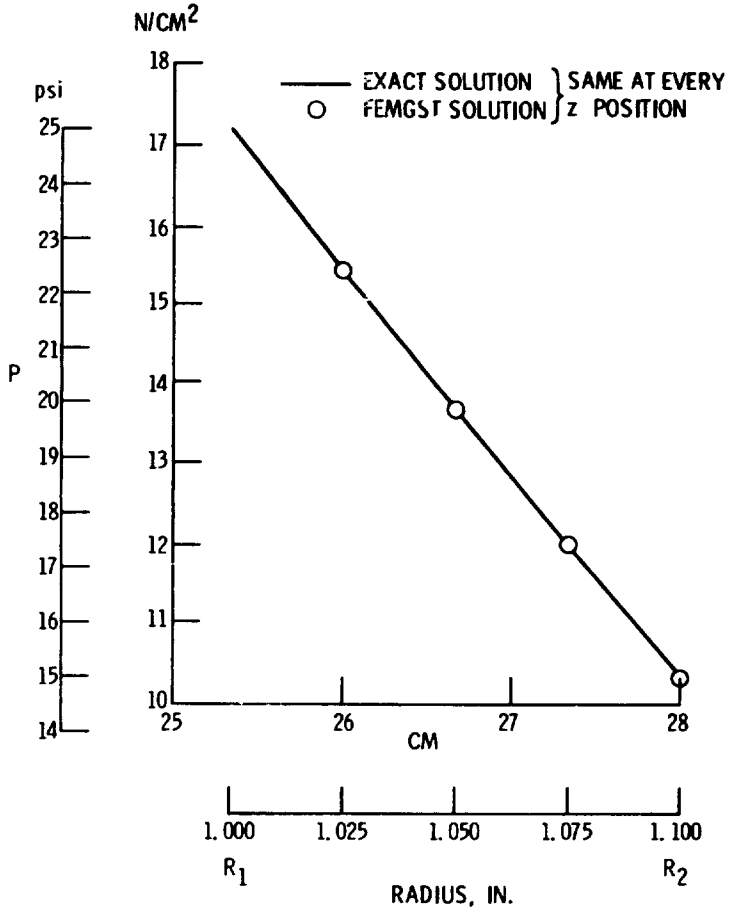


Figure 10. - Comparison of FEMGST solution with exact solution for pressure distribution

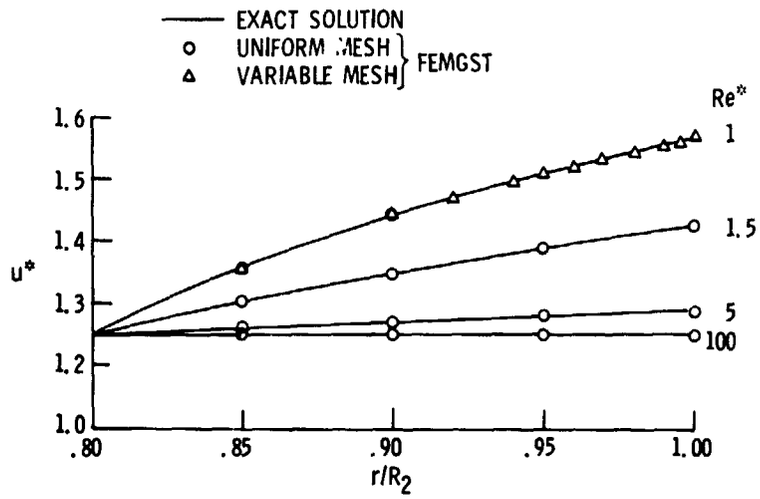


Figure 11. - Comparison of exact inviscid flow solution with FEMGST for velocity distribution and $Re^* = 1, 1.5, 5,$ and 100.

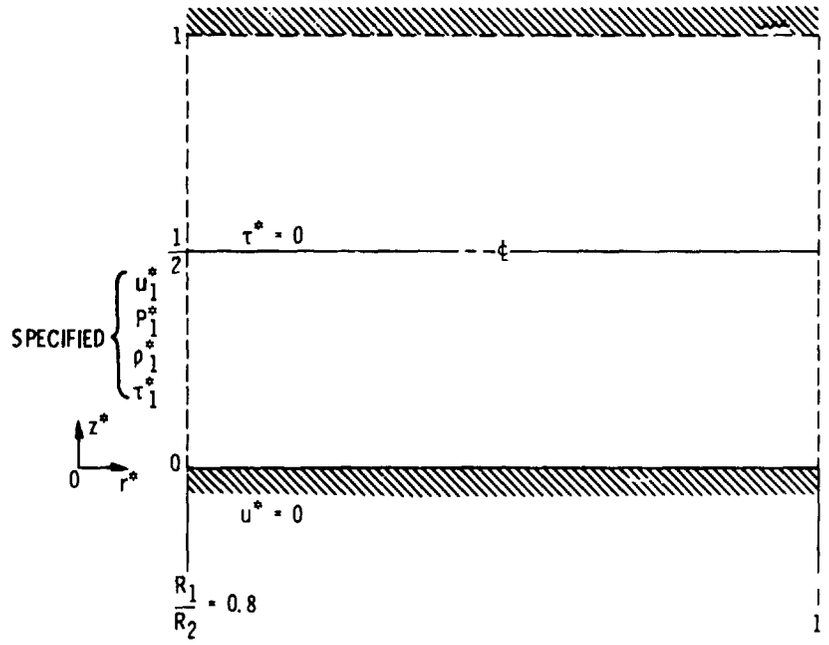


Figure 12. - Domain and boundary conditions for compressible seal leakage problem.

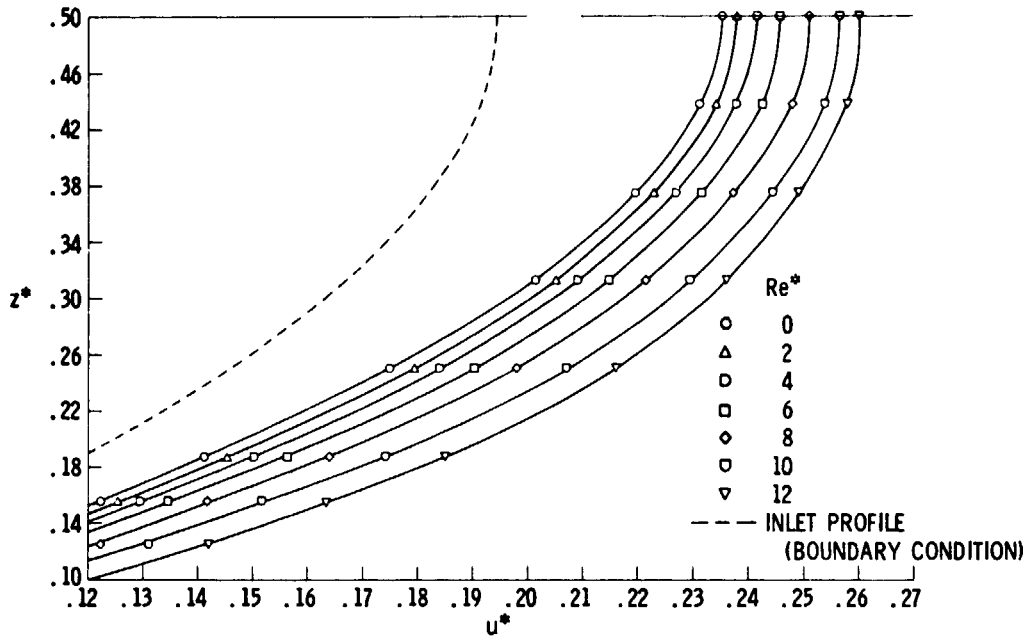


Figure 13. - FEMGST solution for exit velocity profile for a range of Reynolds numbers (0-12); 11 x 17 uniform mesh.

E-5116-2

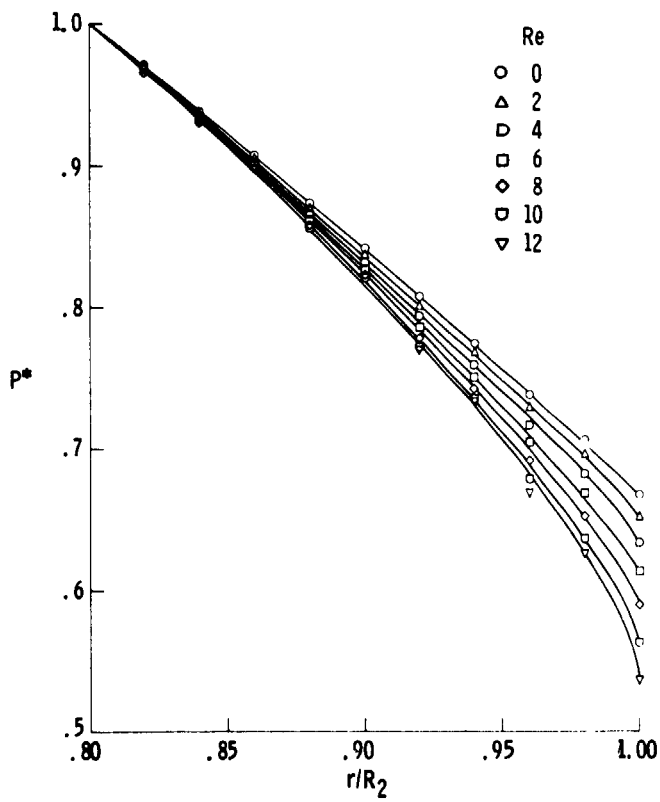


Figure 14. - FEMGST solution for radial pressure distribution at an axial location of $z^* = 0.2500$ for a range of Reynolds numbers (10-12).

NASA-Lewis